VOL. 14, NO. 16, AUGUST2019 ISSN 1819-6608
ARPN Journal of Engineering and Applied Sciences

www.arpnjournals.com

EFFECT FACTORS OF STRUT STRENGTH FOR REINFORCEMENT DEEP BEAMS

Eyad. K. Sayhood and Nisreen S. Mohammed
Department of Civil Engineering, University of Technology, Baghdad, Iraq
E-Mail: nisreen_alnimer@yahoo.com

ABSTRACT

The strut efficiency factor (β_s) is an important for the strength of concrete for the analysis and design of reinforced deep beams based on the strut and tie model. Because of ACI 318M-14 code uses constant values for strut efficiency factor β_s,the proposed empirical formulas used to evaluate the strut efficiency factor B_s will be based on the effect of manyparameters (f_c'), the shear span to effective depth ratio of beams (a_v/d), longitudinal reinforcement percentage (ρ_s), horizontal reinforcement percentage (ρ_h), vertical reinforcement percentage (ρ_v), yield strength of reinforcement (f_y), and effective depth (d). A 121 reinforced deep beams from the literature are used in this study to predict the proposed equation that have minimize the mean absolute error (MAE), root mean square error (RMSE) and maximize the coefficient of multiple determinations (R^2). A good results with the experimental strut efficiency factor and proposed models as it has ($R^2$is range 0.979 to 0.982).

Keywords: shear capacity; strut strength factor, strut and tie, deep beams, span- depth ratio; and compressive strength of concrete.

1. INTRODUCTION

Deep beams are structural elements loaded as simple beams in which a significant amount of the load is carried to the supports by a compression force combining the load and the reaction. This occurs if a concentrated load acts closer than about 2d to the support, or for uniformly loaded beams with a span-to-depth ratio, l_n/d, less than about 4 to 5. [1].

A deep beam is characterized by the ratio of the loading arm (centerline distance between the load and the reaction (a_v) or total span (ln) to the depth of the member (d). The basis for this definition is that within a distance of 'd'from a disturbance such as a concentrated load or support, the strain distribution in the member is nonlinear (St. Venant's principle, Schlaich *et al*., 1987) [2]. Plane sections do not remain plane. Regions of nonlinear strain distribution along the height of the cross-section are called D-regions where 'D' stands for discontinuity or disturbed. Regions of linear strain distribution are called B-regions where 'B' stands for Bernoulli or beam.

Strut-and-tie modeling is currently recommended for the design of reinforced concrete deep beams that replaces complex states of stress with simple, uniaxial stress paths (Schlaich *et al*., 1987) [2]. The flow of forces through a structure is modeled with a collection of compression elements (struts) and tension elements (ties). The intersection of struts and ties are called nodes. The collection of struts, ties, and nodes is considered to be a strut-and-tie model (STM).

Strut-and-tie modeling was adopted as the preferred method of deep beam design by the AASHTO LRFD Bridge Design Specifications-2007 [3] and ACI Building Code (ACI 318M-2014) Appendix A [1].

The total number of reinforced concrete deep beam failed in shear tests is 121 from literature's [9-20] was used to propose empirical formula to evaluate the strut efficiency factor βs and will be based on bearing pressure to allowable stress ratios on each side of nodal zone. The effects of (f_c'), the shear span to effective depth ratio of beams (a_v/d), longitudinal reinforcement percentage (ρ_s), horizontal reinforcement percentage (ρ_h), vertical reinforcement percentage (ρ_v), yield strength of reinforcement (f_y), and effective depth (d) were studied from literature's.

In this study, a modify strut efficiency factor βs adopted in the strut-and-tie model presented in the ACI 318M-14 Code provisions is predicted. The effective strength capacity of diagonal strut for reinforced concrete deep beams was based on available existing experimental data. The reduced capacity of the concrete strut is verified by comparing the predicted efficiency factor with the proven one calculated from existing experimental results.

2. Strut and Tie Model

Strut-and-tie models was evolved in the early 1980s in Europe (Schlaich *et al*., 1987) [2] and ACI318M-14 [1] Section 11.1.1 allows D-regions to be designed using strut-and-tie model according to the provisions of *Appendix A*.

A strut-and-tie model for a deep member is shown in Figure-1. It consists of concrete struts with total number greater than ore qual to the number of supports, longitudinal reinforcement serving as a tension tie, and joints referred to as nodes. The concrete around a node is called nodal zone. The nodal zones transfer the forces from the inclined struts to other struts, to ties and to the supports as reactions.

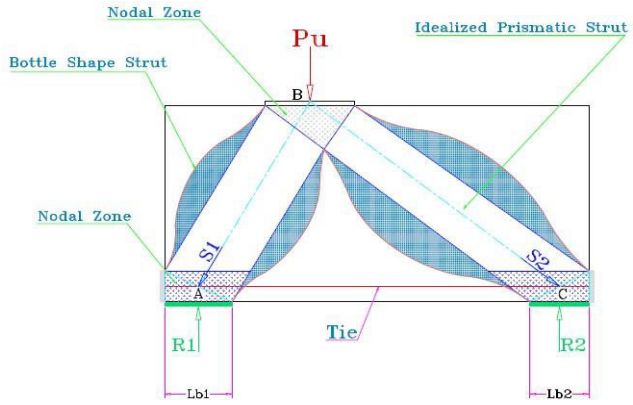

Figure-1. Basic Strut and Tie Model of a Deep Member, Wight and Mac Gregor, 2012 [4].

3. Compression Failure of Strut

The crushing strength of the concrete in a strut is referred to as the effective strength (f_{cu}), where:

$$f_{cu} = \upsilon . f_c' \quad \ldots\ldots\ldots (1)$$

in which ν is an efficiency factor having a value (0-1). ACI318M-14 Section A.3.2 replaces f_{cu} with the effective compressive strength, f_{ce}. The major factors affecting the effective compression strength are:

3.1 The concrete strength.

Concrete becomes more brittle and ν tends to decrease as the concrete strength increases.

3.2 Load duration effects

The strength of concrete members tends to be less than the cylinder compressive strength. f_c' Various reasons are given for this lower strength, including the observed reduction in compressive strength under sustained load, the weaker concrete near the tops of members due to vertical migration of bleeding water during the placing of the concrete, and the different shapes of compression zones and tested cylinders. For flexural members, ACI318M-14 Section 10.2.7.1 accounts for this, in part, by taking the maximum stress in the equivalent rectangular stress block as $0.85f_c'$. For struts, load duration effects are accounted for in the ACICommittee318 by rewriting equation (1) as:

$$f_{ce} = \beta_s.(0.85f_c') \quad \ldots\ldots\ldots (2)$$

Nodal zones are treated similarly except that β_s is replaced by β_n.

3.3 Tensile strains transverse to the strut

These strains result from tensile forces in the reinforcement crossing the cracks, Collins and Mitchell, 1980[5], and Ramirez and Breen, 1991 [6]. In tests of uniformly strained concrete panels, such strains were found to reduce the compressive strength of the panels. The AASHTO specification bases f_{ce} on the concept of AASHTO, LRFD Bridge Specifications, 2007 [3].

3.4 Cracked struts

Struts crossed by cracks inclined to the axis of the strut are weakened by the cracks. ACI318M-14 Section A.3.1 presents the nominal compressive strength of a strut as:

$$\begin{cases} \phi F_{ns} \geq F_{us} \\ F_{ns} = f_{ce}.A_c \end{cases} \quad \ldots\ldots (3)$$

where the subscript n means nominal, s means strut, A_c is the cross-sectional area at the end of the strut, and f_{ce} is as given in Equation (2) above. Values of β_s are given in Table-1. These values were derived byACICommittee318M-2014[1].

Table-1. Values of β_s Strut by ACI Committee 318M-2014 [1].

Strut		
1	For Struts in which the area of the midsection cross section is the same as the area at the nodes, such as the compression zone of a beam or footing. ACI Section A.3.2.1	β_s=1.0
2	For Struts located such that the width of the midsection of the strut is larger than the width at the nodes (Bottle-Shape struts). ACI Section A.3.2.2	
	a- With reinforcement satisfying A.3.3	β_s=0.75
	b- Without reinforcement satisfying A.3.3	β_s=0.6*
3	For Struts in tension members or the tension flanges of members.ACISectionA.3.2.3	β_s=0.4
4	For all other cases.ACISectionA.3.2.4	β_s=0.6λ
*:-In mass concrete members such as pile caps for more than two piles, it may be difficult to place the crack control reinforcement. ACI Code specifies a lower value of f_{ce}. Because the struts are assumed to fail shortly after longitudinal cracking occurs. λ:-Is the correction factor for light weight concrete. λ=1.0for normal weight concrete and 0.75 for all light weight concrete. Otherwise, λ shall be determined based on volume tric proportions of light weight and normal weight aggregates as specified in8.6.1, but shall not exceed 0.85.		

4. Strength Capacity of Ties

The second major component of a strut-and-tie model is the tie. A tie represents one or several layers of reinforcement in the same direction. The design is based on:

$$\phi F_{nt} \geq F_{ut} \quad \ldots\ldots (4)$$

where the subscript *t* refers to "tie" and F_{nt} is the nominal strength of the tie.

At the ultimate limit state, it is supposed that the reinforcement attains the design stress:

4.1 For reinforcing steel

$$\sigma_s = f_y \quad \ldots\ldots. (5)$$

When compatibility conditions are not explicitly studied, it will be necessary to limit the maximum strain in the ties at the ultimate limit state, and thus the stress in thereinforcementisindirectlylimitedattheserviceabilitylimits tate. The nominal strength capacity of a tie may be expressed as follows:

$$F_{nt} = A_s . f_y \quad \ldots. (6)$$

where A_S is the area of reinforcing steel. ACI318M-14 Section A.4.2 requires that the axis of the reinforcement in a tie coincide with the axis of the tie. In the layout of a strut-and-tie model, ties consist of the reinforcement plus a prism of concrete concentric with the longitudinal reinforcement making up the tie. The width of the concrete prism surrounding the tie is referred to as the effective width of the tie; W_{tie}. The lower limit is a width equal to the twice the distance measured from the surface of the concrete to the centroid of the tie reinforcement. In a hydrostatic C-C- Tnodal zone defined in the next section, the stresses on all faces of the nodal zone should be equal. ACI318M-14 Commentary Section R.A.4.2 gives a practical upper limit of the tie width W_{tie} corresponding to the width in a hydrostatic nodal zone, calculated as follows:

$$W_{tie,max.} = \frac{F_{nt}}{f_{ce} . b_w} \quad \ldots\ldots (7)$$

The concrete is included in the tie to establish the widths of nodal zones faces acted on by ties. The concrete in a tie does not resist any load. It aids in the transfer of loads from struts to ties or to bearing areas through bond with the reinforcement. The concrete surrounding the tie steel increases the axial stiffness of the tie by tension stiffening. Tension stiffening may be use din modelling the axial stiffness of the ties in a serviceability analysis.

Ties may fail due to lack of end anchorage. The anchorage of the ties in the nodal zones is a critical part of the design of a D-region using a strut-and-tie model. Ties are normally shown as solidlines in strut-and-tie models. For suitable control of the stress under serviceability conditions and, consequently, of cracking, it is recommended that maximum deformation of the tie steel be limited to 0.2% when a detailed compatibility study is not performed. This involves limiting the total reinforcing steel stress to (f_y≤420MPa), Wight and Mac Gregor, 2012[4].

5. Strength Capacity of Nodes and Nodal Zones

The points at which the forces in struts-and-ties meet in a strut-and-tie model are referred to as nodes. Conceptually, they are idealized as pinned joints. The concrete in and surrounding a node is referred to as a nodal zone. In a planar structure, three or more forces must meet at a node for the node to be in equilibrium, as shown in Figure-2. This requires that:

$$\sum F_x = 0 \ , \sum F_y = 0 \ \& \sum M = 0 \quad \ldots\ldots. (8)$$

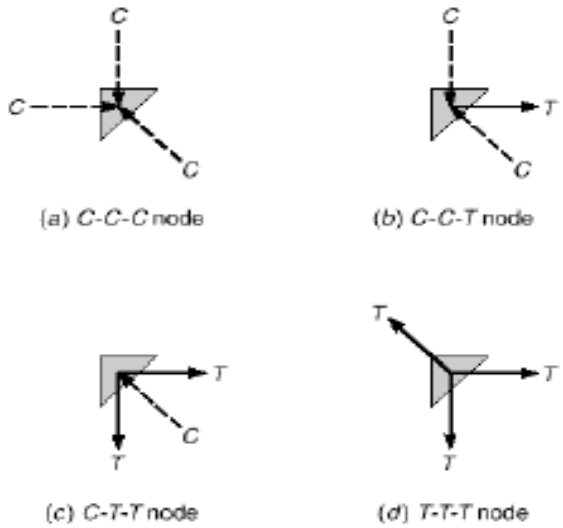

Figure-2. Forces Acting on Nodes, Wight and Mac Gregor, 2012 [4].

The $\Sigma M=0$ condition implies that the lines of action of the forces must pass through a common point, or must be able to be resolved in to forces that act through a common point. Nodal zones are classified as *C-C-C* if three compressive forces meet and as *C-C-T* if on eof the forces is tensile. *C-T-T* and *T-T-T* joints may also occur as shown above. Nodal zones are assumed to fail by crushing. Anchorage of the tension ties is a matter of design consideration. If a tension tie is anchored in a nodal zone there is a strain in compatibility between the tensile strains in the bars and the compressive strain in the concrete of the node. This tends to weaken the nodal zone. ACI318M-14SectionA.5. 1limits the effective concrete strengths, for nodal zones as follows:

$$F_{nn} = f_{ce} . A_n \quad \ldots (9)$$

where A_n is the area of the face of the node that the strut or tie acts on, taken perpendicular to the axis of the strut or tie, or the area of a section through the nodal zone, and f_{ce} is the effective compression strength of the concrete:

$$f_{ce} = \beta_n(0.85f'_c) \quad \ldots\ldots (10)$$

ACI318M-14 Section A.5.2 gives the following three values of β_n fornodal zones listed in Table-2 below:

Table-2. Values of β_n for Nodal Zones by ACI Committee 318.

Nodal Zones		
1	**In nodal zones bounded on all sides by struts or bearing areas, or both. ACI Section A.5.2.1**	$\boldsymbol{\beta_n}$**=1.0**
2	In nodal zones anchoring a tie in one direction. ACI Section A.5.2.2	β_n=0.8
3	In nodal zones anchoring two or more ties. ACI Section A.5.2.3	β_n=0.6

In general, nodes shall be designed, dimensioned and reinforced in such a way that all the acting forces are balanced and the ties are properly anchored. The concrete at the nodes may be subjected to multi-stress states, and this fact will also be taken into account since it implies either an increase or decrease in its strength capacity.

5. Evaluation of Strength Efficiency Factor for Strut-β_s

Key parameter in the analysis and design of concrete elements using strut-and-tie models according to ACI318M-14 [1] Code is the definitions of a strut effective strength factor used to calculate strut strength. In the ACI Code strut effective strength factor β_s is meant to capture the lower compressive strength of concrete when the strut is subjected to off – axis tensile strains. It depends on strut geometry and transverse strain conditions. The total applied force to the deep beams resulted in shear forces transferred to each support. The force in the direct strut forming between load and support in strut-and-tie model, $F_s$is:

$$F_s = \frac{V_u}{\sin\theta} \quad \ldots\ldots (11)$$

where

V_u: is the ultimate shear strength.
θ: is the angle of inclination of the strut.

The top-node height $h_1$and the bottom-node height W_{tie} (Figure-3) can be found as follows:

$$h_1 = \frac{F_s * \cos\theta}{0.85\, f'_c * \beta_n * h_w} \quad for\ \beta_n = 1.0 \quad C-C-C\ Node$$

$$W_{tie} = \frac{F_s * \cos\theta}{0.85\, f'_c * \beta_n * l_w} \quad \text{for } \beta_n = 0.8 \quad C-C-T\ \text{Node} \quad \ldots\ldots (12)$$

Where β_n is increasing degree of disruption of the nodal zones see Table-2, h_w is the transverse dimension of column (load) nodal zone, and l_w is the transverse dimension of support (reaction) nodal zone. Figure-3 shows forces and geometry of nodal zones in the strut-and-tie model. In the present study, the top and bottom nodal zone send in gup the strut are investigated to determine the strut efficiency factor β_s. Even when the support width l_b is wider than half the top bearing plate or (column width b_c), the bottom nodal zone is governing the determination of the strut strength in all specimens.

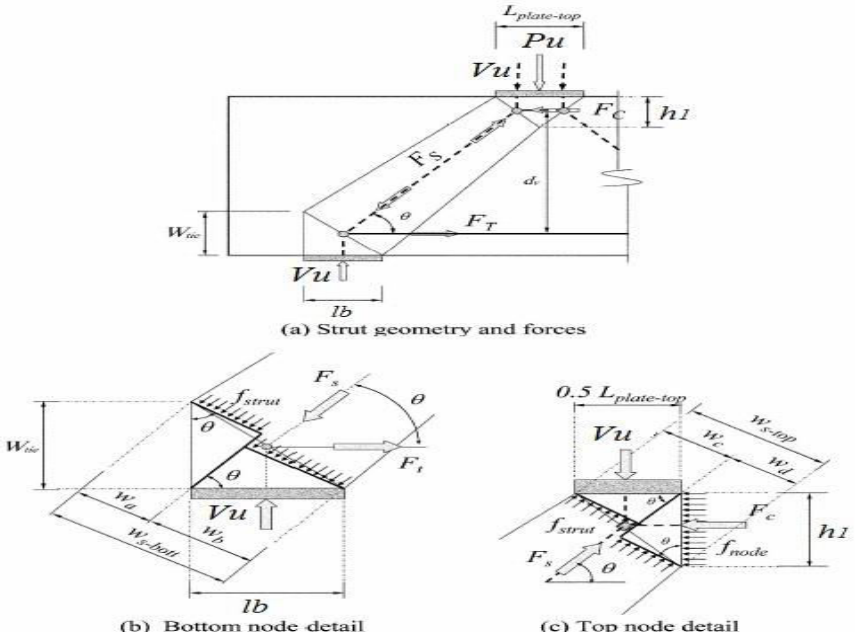

Figure-3. Node Geometry for Strut Strength- β_S, Breñaand Roy, 2009[7].

This is consistent with the location of expected concrete spalling near the top of the strut failed by strut crushing, Breña and Roy, 2009 [7]. Therefore, the top and bottom widths of the strut will be determined as follows:

$$W_{s-top} = \frac{l_{plate}}{2} * \sin\theta + h_1 * \cos\theta$$
$$W_{s-bott.} = l_b * \sin\theta + W_{tie} * \cos\theta \quad \ldots\ldots(13)$$

The stress at the top and bottom ends (i.e. nodal zones) of the strut can be calculated using the following expressions:

$$f_{strut} = \frac{F_s}{W_{s-top} * h_w}$$
$$f_{strut} = \frac{F_s}{W_{s-bott.} * l_w} \quad \ldots\ldots(14)$$

where h_w and l_w are transverse dimensions of column(load plate) and support plate respectively. Where usually l_w and h_w equal to the width of deep beam section (b_w).

By equating the lower stress of strut from the above equations with the ACI 318M-14strut strength (equation 2) to estimate the strut effective strength factor β_S, using equations 11, 12, 13 and 14.

$$\beta_s = \frac{f_{strut}}{0.85\, f_c'}$$
$$\beta_s = \frac{V_u * \beta_n}{0.85\, f_c' \beta_n * (l_w * \sin\theta)^2 + V_u * \cos^2\theta} \quad \ldots\ldots(15)$$

At the next section, Table-5 shows the widths of the strut and tie at bottom nodal zone (W_{tie} &W_s), allowable compressive stress of strut f_{strut}, and effective strength factor $\beta_{s-exp.}$ of strut for a 121 reinforced deep beams from the literature [8-19] failed in shear test,

7. Proposed Expression for Strut Efficiency Factor-β_S

The strut efficiency factor β_S is directly proportional to transverse shear reinforcement ρ_V and longitudinal flexural reinforcement ρ_S, while it is inversely proportional to the ratio of shear span to effective depth ratio (*av/d*) and concrete compressive strength *f'c*. The ACI318M-14 Code values for the strut efficiency factor β_S do not account for the parameters studied in the previous section because the Code uses constant values for this factor. Therefore, it can be noticed that the use of current strut-and-tie modeling provisions of ACI318M-14 leads to estimation of strut efficiency factor β_S. The propos all involves construction of a new expression for the strut efficiency factor β_S thataccountsforallparametersbasedontestresultsandcompiledexperimental data available in literature. The proposed expression of the factor β_S is a function of the parameters *f'c*, ρ_S, ρ_V, ρ_h and (*av/d*) based on their effects on strut efficiency factor β_S. Therefore the proposed empirical formula used to evaluate the strut efficiency factor $\beta_S$will be based on bearing pressure to allow able stress ratios one ach side of bottom nodal zone. Also, the effect of longitudinal flexural reinforcement ρ_S and transverse shear reinforcement (ρ_V&ρ_h) is included in combination with the effect of shear span to effective depth ratio (*av/d*). Hence, the following simple expressions are proposed:

$$\beta_s = [A * R_1 + B * R_2 + C * R_3 + D * R_4]^E$$
$$\beta_s = [A * R_1 + B * R_2 + C * R_3 + D * R_4 + F]^E$$
$$\beta_s = [A * R_1 + B * R_2 + C * R_3 + D * R_4]^E + F$$
$$\beta_s = [A * R_1 + B * R_2 + C * R_3 + D * R_4 + F]^E + G$$

Where:

$$R = \frac{Bearing\ pressure}{Allowable\ stress}$$

$$R_1 = \frac{V_u}{0.85\ f'c\ \beta_n l_b b_w}$$

$$R_2 = \frac{V_u}{0.85\ f'c\ \beta_n\ b_w W_s \sin\theta}$$

$$R_3 = \frac{V_u}{\rho_s b_w\ d\ f_y\ \tan\theta}$$

$$R_4 = \frac{V_s}{0.275\ f'c\ b_w W_s\ (1 - \frac{W_s}{b_{ef}})}$$

Where:

$\boldsymbol{R_1}$ = is the ratio of bearing pressure to allowable stress at support face of bottom nodal zone.

$\boldsymbol{R_2}$ =is the ratio of bearing pressure to allowable stress at strut face of bottom nodal zone.

$\boldsymbol{R_3}$ =is the ratio of tie stress to allowable stress for tie steel reinforcementat bottom nodal zone.

$\boldsymbol{R_4}$ = is the ratio of transverse shear reinforcement stress to allowable stress.

An expression for determining effective width of bottle-shaped strut $b_{ef.}$ shown below in Figure-4 was given by Brown and Bayrak, 2008 [8]:

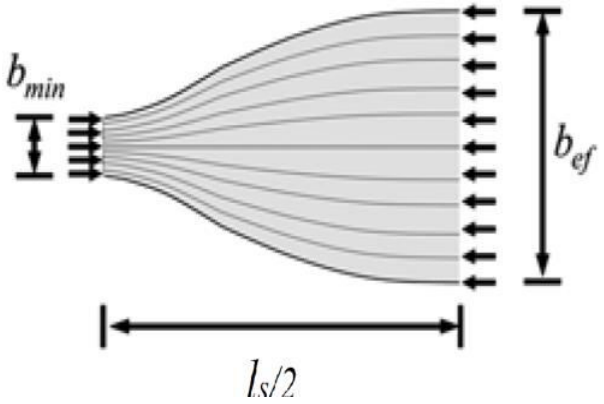

Figure-4. Bottle-Shaped Dispersion of Compression-Elastic Distribution.

$$b_{ef} = \left(b_{min} + \frac{l_s}{6}\right) \geq \frac{h_w}{3} \quad \ldots\ldots(16)$$

where

b_{ef} = is the effective width of Bottle-Shaped strut (i.e. width at mid length

l_s = is the strut length.

b_{min} = is the minimum width at ends of strut.

The maximum possible effective width will be governed by the depth of deep beam and inclution of strut as follows:

b_{ef} = Depth of deep beam/tanθ

V_s = is a shear strength contributed by shear reinforcement.

$$V_s = [\rho_v * k_v + \rho_h * k_h] * f_y * b_w * d \quad \ldots\ldots(17)$$

$$k_v = \frac{1 + (a_v/6)}{6}$$

$$k_h = \frac{5 - (a_v/6)}{6}$$

The coefficients and exponential (A-G) of the proposed formulas are obtained by nonlinear regression analysis. Using these formulas after substituting the test results of ultimate shear strength for the selected 121 deep beams instead ofV_u in these formulas. SPSS statistics-23 program has been used to perform the regression analysis. Table-3 shows values of the coefficients and the final shape of the formulas after adjusting the coefficients to simple values that do not have effect on their accuracy.

Table-3. Coefficients & exponential of the proposed empirical equations.

Proposed equation	A	B	C	D	E	F	G
1	0.88	-0.08	0.08	-0.002	0.815	-	-
2	0.88	-0.08	0.08	-0.002	0.753	-0.025	-
3	0.88	-0.08	0.08	-0.002	0.798	-0.006	-
4	0.88	-0.08	0.08	-0.002	0.655	-0.121	0.045

The final formulas of proposed empirical equations to predict the Strut Efficiency Factor- B_s is:

$$\beta_s = [0.88 * R_1 - 0.08 * R_2 + 0.08 * R_3 - 0.002 * R_4]^{0.815} \quad \ldots\ldots(18)$$

$$\beta_s = [0.88 * R_1 - 0.08 * R_2 + 0.08 * R_3 - 0.002 * R_4 - 0.025]^{0.753} \quad \ldots.(19)$$

$$\beta_s = [0.88 * R_1 - 0.08 * R_2 + 0.08 * R_3 - 0.002 * R_4]^{0.798} - 0.006 \quad \ldots\ldots.(20)$$

$$\beta_s = [0.88 * R_1 - 0.08 * R_2 + 0.08 * R_3 - 0.002 * R_4 - 0.121]^{0.655} + 0.045 \quad \ldots.(21)$$

The error values will be calculated to investigate the accuracy and the performance of each proposed formula. Three additional statistical parameters are selected to make the comparison between the results of experimental work of each proposed formula. These include mean absolute error (*MAE*), root mean square error (*RMSE*) and coefficient of multiple determinations (R^2), these coefficients can be obtained using the following expressions:

$$\mathrm{MAE} = \frac{1}{N}\sum_{i=1}^{N}|x_i - y_i|$$

$$\mathrm{RMSE} = \sqrt{\frac{\sum_{i=1}^{N}(x_i - y_i)^2}{N}}$$

$$R^2 = 1 - \frac{\mathrm{SSE}}{\mathrm{SST}} = 1 - \frac{\sum_{i=1}^{N}(x_i - y_i)^2}{\sum_{i=1}^{N}(x_i - \bar{x})^2}$$

Where

SSE measures the "unexplained" variation (the sum of the squares of the residuals).

SST measures the variation in the experimental or observed shear strength.

$\mathbf{x_i}$ is the experimental value of shear strength for a certain deep beams.

$\bar{\mathbf{x}}$ is the average value of experimental values for all deep beams.

$\mathbf{y_i}$ is the predicted value of shear strength for a certain deep beams.

The (*MAE*) represents the average over the verification sample of the absolute values of the differences between predicted and the corresponding observation. The (*MAE*) is a linear score which means that all the individual differences are weighted equally in the average.

The (*RMSE*) represents the difference between predicted and corresponding observed values, in which they are squared and then averaged over the sample; the square root of the average is taken. The (*MAE*) and the (*RMSE*) can be used together to diagnose the variation in the errors in a set of predicted values. The (*RMSE*) will always be larger than or equal to the (*MAE*); the greater the difference between them, the greater the variance in the individual errors in the sample. If the (*RMSE=MAE*), then all the errors are of the same magnitude. Both the (*MAE*) and (*RMSE*) can range between 0 and ∞. They are negatively-oriented scores, where lower values are better. The coefficient of multiple determinations (R^2) measures the proportion of variation in the data points which is explained by the regression model. A value of (R^2=1) means that the curve passes through every data points, while a value of ($R^2 = 0$) means that the regression models do not describe the data any better than a horizontal line passing through the average of the data points, The proposed models that minimize the mean absolute error (*MAE*) and root mean square error (*RMSE*) and maximize the coefficient of multiple determinations (R^2) are selected as optimum empirical equations. Table-4 shows the superiority of proposed models over those cited in the literature based on a number of nonlinear iterations, (*MAE*), (*RMSE*) and (R^2). After regression analysis process, the resulting equations are used to analyze the deep beams considered in this study. All equations show excellent accuracy of fitting (R^2) closer to unity. This reflects the reasonable accuracy of these equations in comparison with the existing empirical equations. For detailed comparison between the proposed equations and existing equations, only equation of Proposal 4 is selected, as it have the minimum values of (*MAE*) and (*RMSE*) engaged with maximum values for coefficient of multiple determinations (R^2). These results illustrate the accurate convergence between test results and analytical results by using these two equations because all ratios are generally close to unity for all deep beams.

Table-4. Fitting accuracy of proposed empirical equations to predict the Strut Efficiency Factor- B_s.

Proposal No.	(MAE)	(RMSE)	(R^2)
4	0.01191771	0.01701771	0.98249995
2	0.01277098	0.01804635	0.98032042
3	0.01301066	0.01819859	0.979987
1	0.01320136	0.01824332	0.97988849

Table-5 gives values of (β_S) *Exp* using eq. (15), (β_S) *ACI* adopted by the ACI318M-14 Code and (β_S) *Pre.* Which is proposed here (proposal No. 4)? This table shows that the results of proposed equation are very close to the

experimental results, while the ACI318M-14 Code values are not consistent with the experimental results. Also, Figure-5 shows a comparison between experimental from literature's [9 - 2 0] and theoretical results obtained by the ACI318M-14 Code and by the proposed equation for effectiveness factor ($\beta_s)Pre$. It shows that the proposed equation has good agreement with test results where the data points of the proposed equation are convergent among themselvesandareclosetothe45° line (β_s) $Exp.=(\beta_s)Pre.$), while the ACI318M-14 Code provisions give un-conservative results as their data points have large dispersant away from the 45^{o}line.

Table-5. Model Parameters for Strut Strength Evaluation of the Tested Deep Beams, ACI 318M-14[1] with the Experimental, and Proposed Values of Strut Factor - B_s.

Ref	Deep beam No.	$f'c$	av/d	Exp. Ultimate shear Load Vu (KN)	Strut Angle ɵ°	Node Height W_{tie} (mm)	Strut Width W_s(mm)	f_{strut} (Mpa)	β_{s-exp} eq. 15	$\beta_s)ACI$	$\beta_s)pre$ eq. 21
(8)	DB-1	18.5	0.42	178.0	56.5	76	138	10.6	0.678	0.75	0.688
	DB-2	21.0	0.42	225.0	56.5	76	138	13.0	0.733	0.75	0.748
	DB-3	22.0	0.42	235.0	56.5	76	138	13.6	0.731	0.75	0.745
	DB-4	21.5	0.42	200.0	56.5	76	138	12.0	0.661	0.75	0.671
	DB-5	21.7	0.42	205.0	56.5	76	138	12.3	0.668	0.75	0.68
	DB-6	20.8	0.42	218.0	56.5	76	138	12.7	0.721	0.75	0.735
	DB-7	20.0	0.42	191.0	56.5	76	138	11.4	0.674	0.75	0.685
	DB-8	18.5	0.906	130.0	48.2	76	113	11.2	0.694	0.75	0.681
	DB-9	21.0	0.906	165.0	48.2	76	113	13.4	0.742	0.75	0.748
	DB-10	21.0	0.906	187.0	53.3	76	125	13.1	0.706	0.75	0.71
	DB-11	21.5	0.906	150.0	48.2	76	113	13.0	0.691	0.75	0.678
	DB-12	21.3	0.906	149.0	48.2	76	113	12.9	0.692	0.75	0.68
	DB-13	20.9	0.906	146.0	48.2	76	113	12.6	0.691	0.75	0.679
	DB-14	20.0	0.906	143.0	48.2	76	113	12.2	0.701	0.75	0.69
(9)	DB-15	34.5	0.64	449.7	52.6	117	192	20.4	0.702	0.75	0.708
	DB-16	34.5	0.64	465.2	52.6	117	192	20.9	0.719	0.75	0.726
	DB-17	34.5	0.76	434.1	53.1	115	191	20.4	0.685	0.75	0.689
	DB-18	34.5	0.76	452.1	53.1	115	191	20.9	0.704	0.75	0.71
	DB-19	34.5	0.94	443.0	53.1	115	188	21.1	0.694	0.75	0.698
	DB-20	34.5	0.94	419.1	53.1	115	188	20.6	0.668	0.75	0.669
(10)	DB-21	40.0	1.83	283.0	55.3	125	189	18.8	0.3	0.6	0.276
	DB-22	40.0	1.83	455.8	58.1	125	198	21.8	0.4	0.75	0.401
	DB-23	34.0	1.21	300.0	45.9	126	179	21.6	0.724	0.75	0.714
	DB-24	29.0	1.21	255.0	45.9	126	179	18.4	0.723	0.75	0.713
	DB-25	22.4	1.78	156.1	54.4	86	130	14.1	0.631	0.75	0.626
	DB-26	26.6	1.78	140.4	54.4	86	130	15.5	0.511	0.6	0.503
	DB-27	23.5	1.78	123.6	54.4	86	130	13.6	0.51	0.6	0.502
(11)	DB-28	34.9	1.85	2563.7	54.1	294	447	19.6	0.481	0.75	0.47
(12)	DB-29	41.0	1.87	348.0	48.8	120	167	22.9	0.477	0.6	0.438
(13)	DB-30	24.0	0.85	275.0	50.4	120	188	15.4	0.747	0.75	0.755
	DB-31	23.7	1.25	228.7	47.3	120	173	15.2	0.725	0.75	0.72
	DB-32	23.7	1.25	255.7	47.3	120	173	15.8	0.773	0.75	0.782
	DB-33	23.7	1.25	208.7	47.3	120	173	14.6	0.687	0.75	0.672
	DB-34	24.0	0.85	270.0	49.8	120	185	15.5	0.749	0.75	0.757

Ref	Deep beam No.	$f'c$	av/d	Exp. Ultimate shear Load Vu (KN)	Strut Angle ɵ°	Node Height W_{tie} (mm)	Strut Width W_s(mm)	f_{strut} (Mpa)	β_{s-exp} eq. 15	$\beta_s)ACI$	$\beta_s)pre$ eq. 21
(14)	DB-35	36.1	1.84	2530.0	56.4	270	460	20.5	0.452	0.75	0.453
	DB-36	36.7	1.84	2922.0	56.4	270	460	21.6	0.501	0.75	0.505
	DB-37	27.2	1.84	2019.0	56.4	270	460	15.7	0.473	0.6	0.476
	DB-38	28.6	1.84	2348.0	56.4	270	460	17.0	0.514	0.6	0.518
	DB-39	24.0	1.84	2150.0	57.4	173	381	16.0	0.747	0.75	0.773
	DB-40	24.0	1.84	2121.0	57.4	173	268	16.0	0.74	0.75	0.746
	DB-41	31.0	1.84	2750.0	57.4	173	561	20.6	0.742	0.75	0.784
	DB-42	23.0	1.84	1480.0	56.9	173	268	14.2	0.592	0.6	0.594
	DB-43	31.9	1.84	1463.0	56.9	173	268	17.8	0.451	0.6	0.45
	DB-44	28.2	1.84	2170.0	66.9	173	381	16.2	0.449	0.6	0.487
	DB-45	28.2	1.84	2295.0	66.9	173	381	16.5	0.472	0.6	0.51
	DB-46	32.0	1.84	1832.0	63.7	173	381	17.5	0.402	0.75	0.433
	DB-47	29.0	1.84	1230.0	63.7	173	381	14.1	0.306	0.6	0.326
	DB-48	22.8	1.84	2095.0	66.9	173	381	13.8	0.528	0.75	0.563
	DB-49	22.8	1.84	2081.0	66.9	173	381	13.8	0.525	0.6	0.561
	DB-50	29.1	1.2	3687.0	66.9	173	445	18.6	0.7	0.75	0.731
	DB-51	28.0	2.49	1350.0	68.5	173	302	14.9	0.265	0.6	0.273
	DB-52	31.2	2.49	2295.0	68.5	173	302	18.6	0.395	0.75	0.42
	DB-53	35.0	1.85	3385.0	52.6	310	604	21.6	0.599	0.6	0.602
	DB-54	34.0	1.85	3745.0	52.6	310	604	21.7	0.657	0.75	0.665
	DB-55	32.5	2.5	2268.0	61.5	310	430	17.9	0.317	0.6	0.312
	DB-56	26.0	1.85	1480.0	63.0	178	344	14.3	0.403	0.75	0.426
	DB-57	27.0	1.85	1560.0	63.0	178	344	14.9	0.408	0.6	0.433
	DB-58	31.9	1.2	2633.0	66.3	178	405	17.3	0.48	0.6	0.519
	DB-59	28.3	1.85	5017.0	45.4	400	627	17.8	0.659	0.75	0.634
	DB-60	20.7	1.85	4136.0	45.4	400	449	13.4	0.706	0.75	0.675
	DB-61	28.3	1.85	6294.0	45.4	400	627	18.7	0.749	0.75	0.752
	DB-62	33.8	1.85	4875.0	45.4	400	627	20.1	0.58	0.75	0.538
	DB-63	28.2	1.85	5016.8	45.0	408	545	17.7	0.66	0.75	0.626
	DB-64	28.2	1.85	6291.6	45.0	408	545	18.7	0.749	0.75	0.742
	DB-65	33.7	1.85	4873.2	45.0	408	545	20.0	0.582	0.75	0.531
	DB-66	20.7	1.85	4135.1	45.0	408	545	13.4	0.706	0.75	0.684
(15)	DB-67	39.0	1.87	350.3	52.5	130	190	20.6	0.4	0.6	0.375
	DB-68	38.0	2.2	215.0	61.9	91	149	17.9	0.234	0.6	0.216

Table-5. Continued.

Ref	Deep beam No.	$f'c$	av/d	Exp. Ultimate shear load Vu (KN)	Strut Angle θ°	Node Height W_{tie}(mm)	Strut Width W_s(mm)	f_{strut} (Mpa)	β_{s-exp} eq. 15	$\beta_s)ACI$	$\beta_s)pre$ eq.21
(16)	DB-69	21.0	0.83	150.0	49.6	102	157	13.2	0.73	0.75	0.732
	DB-70	21.0	0.83	140.0	49.6	102	157	12.7	0.699	0.75	0.694
	DB-71	20.0	0.83	138.0	49.6	102	157	12.3	0.714	0.75	0.712
	DB-72	22.5	0.83	165.0	49.6	102	157	14.3	0.742	0.75	0.746
	DB-73	23.0	0.83	170.0	49.6	102	157	14.7	0.745	0.75	0.75
	DB-74	23.5	0.83	168.0	49.6	102	157	14.8	0.73	0.75	0.731
	DB-75	22.0	0.83	160.0	49.6	102	157	13.9	0.738	0.75	0.74
	DB-76	21.5	0.83	155.0	49.6	102	157	13.6	0.734	0.75	0.734
	DB-77	20.5	0.83	150.0	49.6	102	157	13.0	0.741	0.75	0.742
	DB-78	20.0	0.83	144.0	49.6	102	157	12.6	0.734	0.75	0.73
	DB-79	21.0	0.83	155.0	49.6	102	157	13.4	0.745	0.75	0.744
	DB-80	22.0	0.83	163.0	49.6	102	157	14.1	0.747	0.75	0.746
	DB-81	21.0	0.83	155.0	49.6	102	157	13.4	0.745	0.75	0.744
	DB-82	22.1	1	147.0	49.6	102	155	13.6	0.698	0.75	0.693
	DB-83	20.1	1	143.5	49.6	102	155	12.8	0.73	0.75	0.731
	DB-84	20.8	1	140.0	49.6	102	155	12.9	0.703	0.75	0.699
	DB-85	20.5	1	153.0	49.6	102	155	13.3	0.75	0.75	0.755
	DB-86	19.0	1	128.5	49.6	102	155	11.8	0.706	0.75	0.701
	DB-87	19.0	1	131.0	49.6	102	155	11.9	0.714	0.75	0.711
	DB-88	17.5	1	126.0	49.6	102	155	11.2	0.734	0.75	0.734
	DB-89	21.8	1	150.0	49.6	102	155	13.7	0.713	0.75	0.71
	DB-90	19.8	1	140.0	49.6	102	155	12.6	0.725	0.75	0.724
	DB-91	18.0	1	125.0	49.6	102	155	11.3	0.717	0.75	0.713
	DB-92	21.0	1	155.0	49.6	102	155	13.6	0.745	0.75	0.747
	DB-93	20.5	1	150.0	49.6	102	155	13.2	0.741	0.75	0.741
	DB-94	20.5	1	149.0	49.6	102	155	13.2	0.738	0.75	0.737
	DB-95	21.6	1	160.0	49.6	102	155	14.0	0.746	0.75	0.748
	DB-96	19.0	1	140.0	49.6	102	155	12.3	0.744	0.6	0.75
	DB-97	21.9	1.33	123.0	45.0	102	141	13.9	0.708	0.75	0.689
	DB-98	22.7	1.33	131.0	45.0	102	141	14.5	0.719	0.75	0.703
	DB-99	21.8	1.33	122.0	45.0	102	141	13.8	0.707	0.75	0.687
	DB-100	19.9	1.33	124.0	45.0	102	141	13.0	0.749	0.75	0.745
	DB-101	19.2	1.33	103.5	45.0	102	141	12.0	0.692	0.75	0.667
	DB-102	19.3	1.33	115.0	45.0	102	141	12.5	0.731	0.75	0.72
	DB-103	20.4	1.33	124.5	45.0	102	141	13.3	0.741	0.75	0.733

Table-5. Continued.

Ref	Deep beam No.	$f'c$	av/d	Exp. Ultimate shear load Vu (KN)	Strut Angle θ°	Node Height W_{tie}(mm)	Strut Width W_s(mm)	f_{strut} (Mpa)	β_{s-exp} eq. 15	$\beta_s)ACI$	$\beta_s)pre$ eq. 21
(16)	DB-104	20.8	1.33	124.0	45.0	102	141	13.4	0.732	0.75	0.72
	DB-105	21.0	1.33	140.5	45.0	102	141	14.1	0.778	0.75	0.784
	DB-106	17.1	1.33	120.0	49.6	102	150	11.0	0.722	0.75	0.717
	DB-107	18.3	1.33	127.5	49.6	102	150	11.8	0.719	0.75	0.714
	DB-108	19.0	1.33	133.0	49.6	102	150	12.3	0.721	0.75	0.716
	DB-109	19.6	1.33	140.0	49.6	102	150	12.7	0.73	0.75	0.727
	DB-110	18.6	1.33	128.5	49.6	102	150	12.0	0.715	0.75	0.709
	DB-111	20.0	1.33	145.0	49.6	102	150	13.1	0.737	0.75	0.735
	DB-112	19.5	1.33	144.0	49.6	102	150	12.8	0.745	0.75	0.744
	DB-113	21.2	1.33	150.0	49.6	102	150	13.7	0.726	0.75	0.722
	DB-114	17.3	2	87.0	49.6	102	144	10.4	0.58	0.75	0.553
(17)	DB-115	35.0	0.84	635.0	52.6	210	344	18.5	0.595	0.6	0.59
	DB-116	30.8	1.13	446.0	46.6	232	329	17.1	0.578	0.6	0.538
(18)	DB-117	35.4	1.72	1615.5	65.8	180	347	19.4	0.42	0.75	0.449
	DB-118	35.0	1.72	1592.9	65.8	180	347	19.2	0.419	0.75	0.448
	DB-119	23.0	0.74	127.2	56.5	76	137	14.5	0.733	0.75	0.747
	DB-120	22.5	1.17	77.8	56.5	76	128	12.1	0.511	0.75	0.514
(19)	DB-121	33.0	1.17	335.0	33.4	174	209	20.8	0.747	0.75	0.702

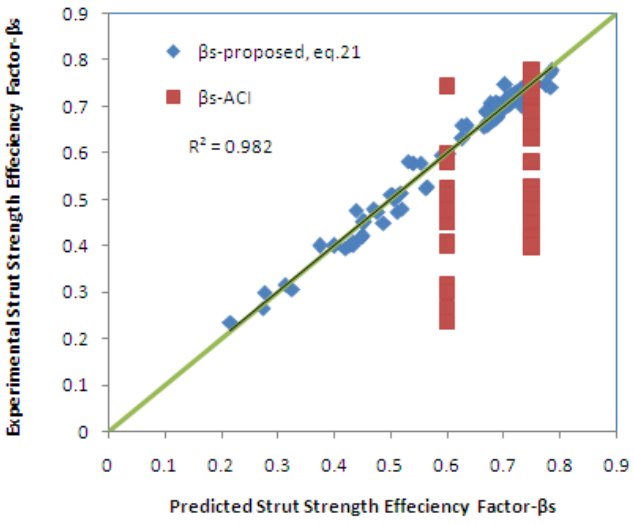

Figure-5. Comparison between Experimental and predicted strut effective strength factors β_s.

8. Effect of Influencing Parameters on Strut Factor-β_S

ACI 318M-14 Building Code incorporate the effectiveness factor β_S which represents the reduction factor for accounting for the effect of lateral tension stress (i.e. off axis stress) on the compression capacity of the strut. The value of this factor is inversely proportional to the tensile stress, so that it decreases with increasing tensile stress. In this section four parameters are studied on which the strut factor β_S depends.

8.1 Effect of concrete compressive strength- f'_c

Figure-6 shows that as the concrete compressive strength f'_c increases the strut effective strength factor β_s decreases where. As the concrete strength increases, the response becomes increasingly brittle. It is evidence that limiting the compressive strength of concrete may enhance ductility, which is crucial to the application of strut- and tie modeling.

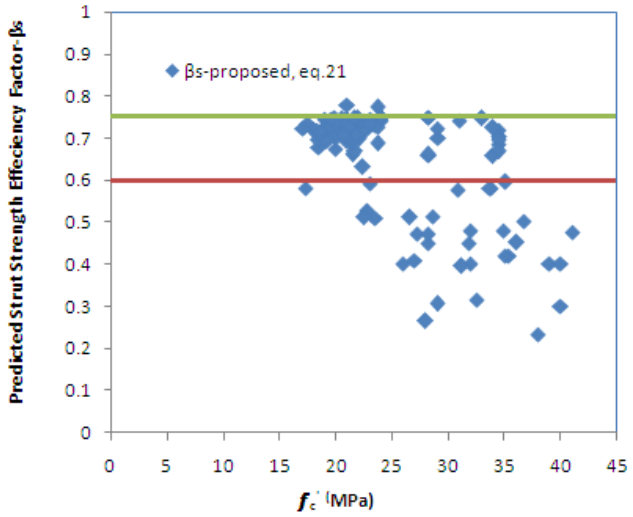

Figure-6. Effect of f'_con strut factor-β_s of deep beams.

8.2 Effect of Shear Span to Effective Depth Ratio-(*av/d*)

Figure-7 shows that the strut effective strength factor $\beta_s$decreases with increasing shear span to effective depth ratio (*av/d*). It is consisting with the presence of higher longitudinal tensile strain developed in tension zone.

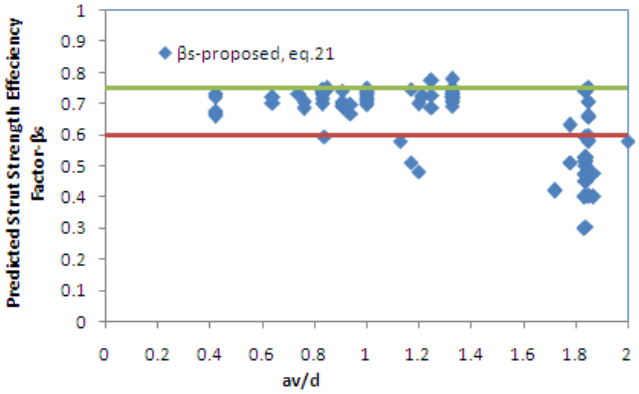

Figure-7. Effect of ***av/d***on strut factor-β_s of deep beams.

8.3 Effect of Shear Reinforcement Ratio-ρ_s,ρ_v&ρ_h

Figures 8 to 10 show that when the longitudinal reinforcement (ρ_s) is increased the strut efficiency factor $\beta_s$increases. This is due to reduction in the tensile stress in the tie reinforcement. As well as the transverse (ρ_v) and horizontal (ρ_h) shear reinforcement is increased the strut efficiency actor β_S increases as they share and carry part of tensile stress with concrete.

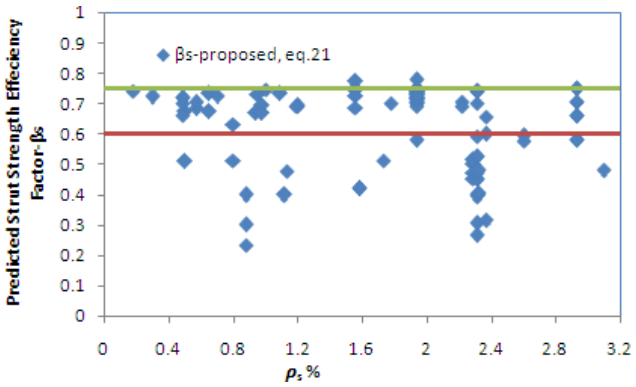

Figure-8. Effect of $\rho_s$on strut factor-β_s of deep beams.

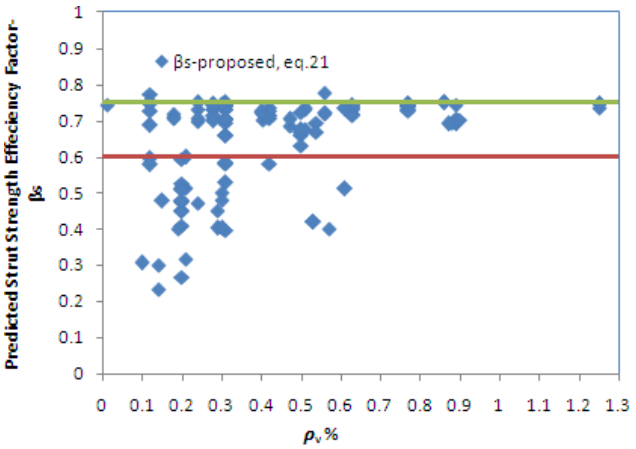

Figure-9. Effect of $\rho_v$on strut factor-β_s of deep beams.

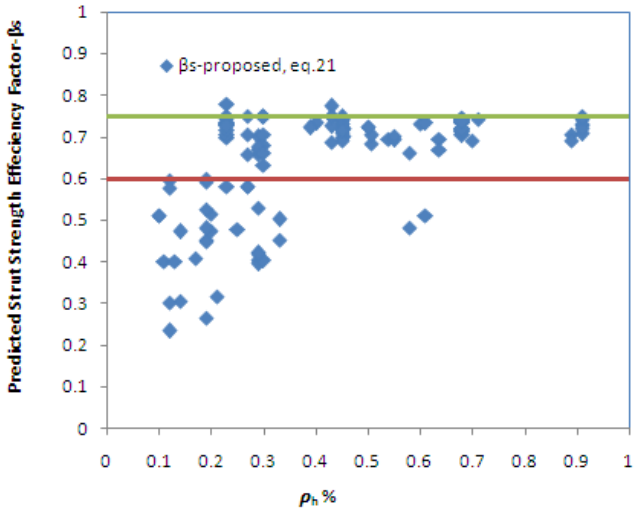

Figure-10. Effect of $\rho_h$on strut factor-β_s of deep beams.

8.4 Effect of yield strength of Reinforcement-f_y

Figure-10 show that when the yield strength of reinforcement $f_y$is increased the strut efficiency factor β_S increases.

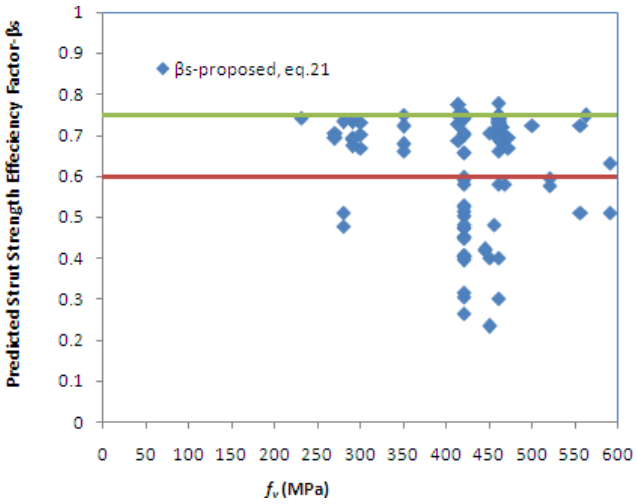

Figure-11. Effect of $f_y$on strut factor-β_s of deep beams.

9. CONCLUSIONS

Based on strut-and-tie model technique of ACI318M-14 Code, anew expression for strut efficiency factor β_S is proposed for deep beams to account for the effects of shear span to effective depth ratio (*av/d*), transverse ρ_v, horizontal $\rho_h$and long itudinal ρ_S reinforcement ratios, and concrete compressive strength *f'c* instead of the provisions of ACI318M-14 which adopts only constant values. This modification in addition to some assumptions makes the proposed expression having better agreement with test results as it has coefficient of multiple determinations (R^2=0.982).

REFERENCES

[1] ACI Committee 318. 2014. Building Code Requirements for Structural Concrete (ACI 318M-14) and Commentary. American Concrete Institute, Farmington Hills, Michigan. p. 503.

[2] Schlaich J., Schafer K. and Jennewein M. 1987. Toward a Consistent Design of Structural Concrete. Journal of the Pre-stressed Concrete Institute. 32(3): 74-150.

[3] AASHTO, LRFD Bridge Specifications, Fourth Edition, American Association of State Highway and Transportation Officials, Washington, 2007.

[4] Wight J., K. and Mac Gregor J. G. 2012. Reinforced Concrete Mechanics and Design. Sixth Edition, Pearson Prentice Hall. p. 1157.

[5] Collins M., P. and Mitchell D. 1980. Design Proposals for shear and Torsion. Journal of the Pre-stressed Concrete Institute. 25(5): 70.

[6] Ramirez, J., and Breen, J., E. 1991. Evaluation of a Modified Truss- Model Approach for beams on Shear. ACI Structural Journal. 88(5): 562-571.

[7] Breña S., F. and Roy, N., C. 2009. Evaluation of Load Transfer and Strut Strength of Deep Beams with Short Longitudinal Bar Anchorage. ACI Structural Journal. 106(5): 678-689.

[8] Brown M., D. and Bayrak O. 2008. Design of Deep Beams Using Strut-and-Tie Models-Part II: Design Recommendations. ACI Structural Journal. 105(4): 405-413.

[9] Abdur Rashid, M. and Kabir, Ahsanul. 1998. Behavior of reinforced concrete Deep beam under uniform loading. Journal of civil engineering, the institution of engineering, Baghdad. CE 24(2):155-169.

[10] Ahmad S., Shah A., Zaman N. and Salimullah K. 2011. Design and evaluation of the shear strength of deep beams by strut and the model (STM). (IJST) Transaction of civil and environmental engineering. 35(C1): 1-13.

[11] Ashour A.F. 2000. Shear Capacity of Reinforced Concrete Deep Beams. Journal of Struct. Eng., ASCE. 126(9): 1045-1052.

[12] Deschenes D. 2009. M. S. Thesis in Progress, University of Texas at Austin, projected completion.

[13] Kong F. K.; Robins P. J. and Cole, D. F. 1970. Web Reinforcement Effects on Deep Beams. ACI JOURNAL, Proceedings. 67(12): 1010-1017

[14] Oh, J. K., and Shin, S. W. 2001. Shear Strength of Reinforced High-Strength Concrete Deep Beams. ACI Structural Journal. 98(2): 164-173.

[15] Robin Garrett Tuchscherer, B. S., M. S. 2008. Strut-and-Tie Modeling of Reinforced Concrete Deep Beams: Experiments and Design Provisions. PhD. thesis, The University of Texas at Austin. p. 298.

[16] Rogowsky D. M.; Mac Gregor, J. G. and Ong, S. Y. 1986. Tests of Reinforced Concrete Deep Beams. ACI Journal. 83(4): 614-623.

[17] Smith K. N. and Vantsiotis A. S. 1982. Shear Strength of Deep Beams. ACI JOURNAL, Proceedings. 79(3): 201-213.

[18] Tan K. H. and Lu H. Y. 1999. Shear behavior of Large Reinforced Concrete Deep Beams and Code Comparisons. ACI Structural Journal. 96(5): 836-845.

[19] Uribe C. M. and Alcocer S. M. 2001. Behavior of Deep Beams Designed with Strutand- Tie Models. Centro Nacional de Prevención de Disastres. p. 247. (In Spanish).

[20] Yang K.H., Chung H.S. and Ashour A.F. 2007. Influence of inclined web reinforcement on reinforced concrete deep beams with openings, ACI Structural Journal. 104(5): 580-589.